

1 *Published in:*

2 **European Journal of Agronomy 123: 126206**

3 <https://doi.org/10.1016/j.eja.2020.126206>

4

5 **A fruit growth approach to estimate oil content in olives**

6 Álvaro López-Bernal^{a,*} (g42lobea@uco.es), Anabela A. Fernandes-Silva^b (anaaf@utad.pt),

7 Victorino A. Vega^c (victorianoa.vega@juntadeandalucia.es), Juan C. Hidalgo^c

8 (jcarlos.hidalgo@juntadeandalucia.es), Lorenzo León^c (lorenzo.leon@juntadeandalucia.es),

9 Luca Testi^d (lucatesti@ias.csic.es), Francisco J. Villalobos^{a,d} (ag1vimaf@uco.es)

10 ^a Departamento de Agronomía, Universidad de Córdoba, Campus de Rabanales, Edificio
11 C4, 14071, Córdoba, Spain

12 ^b Departamento de Agronomia and Centre for the Research and Technology of Agro-
13 Environmental and Biological Sciences, CITAB, University of Trás-os-Montes and Alto
14 Douro, UTAD, Quinta de Prados 5000-801 Vila Real, Portugal

15 ^c Instituto de Investigación y Formación Agraria y Pesquera (IFAPA-Centro Alameda del
16 Obispo), Av. Menéndez Pidal s/n, 14080, Córdoba, Spain

17 ^d Instituto de Agricultura Sostenible (IAS), Consejo Superior de Investigaciones Científicas
18 (CSIC), Av. Menendez Pidal s/n, 14080, Cordoba, Spain

19 *Corresponding author: g42lobea@uco.es

20 **Abstract**

21 Harvest timing in olive orchards has a strong effect on the quality and quantity of oil yield,
22 but many farmers still lack simple and affordable quantitative tools for rationally deciding
23 appropriate harvest dates. This study presents and tests a conceptual model for predicting
24 fruit oil content (O_f , g oil fruit⁻¹) from inexpensive measurements of fruit dry weight (w_f).
25 The model presents two physiologically relevant parameters, the fruit dry weight at the
26 onset of the oil accumulation phase (w_{f0}) and the ratio of accumulated oil per unit of fruit
27 dry weight increase during the oil accumulation period (β), the latter assumed invariable
28 throughout ripening. A compilation of data on w_f and O_f dynamics collected from four
29 experiments including six olive cultivars and contrasting conditions of water supply and
30 crop load was used to test the model. Our results suggest that β could be fairly independent
31 of crop load or watering regime and, probably, genetically controlled. By contrast, w_{f0} is
32 clearly affected by both the cultivar and the availability of assimilates for fruit growth
33 preceding oil accumulation, which makes it orchard- and year-specific. According to those
34 premises, once cultivar-specific β values are available w_{f0} could be easily calibrated by
35 either a single determination of O_f and w_f at any time during the oil accumulation phase
36 (Approach A) or by directly measuring w_{f0} if the date for the onset of oil accumulation can
37 be estimated (Approach B). Validation tests with an independently calibrated β showed an
38 excellent performance for reproducing O_f patterns from w_f data using Approach A.
39 Approach B satisfactory predicted oil accumulation rates, but absolute estimates of O_f were
40 less reliable. Regardless of the calibration approach, the model is easy to implement and
41 has a minimal cost, which satisfies the demand for inexpensive tools for monitoring oil
42 accumulation dynamics.

43

44 **Keywords:** cultivar variability, fruit growth and development, crop modelling, oil
45 accumulation, *Olea europaea* L.

46 **1. Introduction**

47 The recognition of the nutritional characteristics and health benefits of olive oil has led to
48 an increased demand for this product, which has triggered the expansion of this tree crop in
49 the last decades, both in traditional growing regions in the Mediterranean basin and new
50 areas around the world. Covering more than 10 Mha nowadays, olive orchards represent
51 one of the main oil crops worldwide (FAOSTAT, 2017).

52 As in any other oil crop, oil yield results from the product of fruit/seed number, fruit/seed
53 weight and oil concentration at maturity. Understanding the dynamics of these components
54 may be useful for establishing the optimal harvest date, as it is a pivotal agronomical
55 decision that determines the yield and quality of olive oil, the two major revenue
56 determinants in olive orchards (Mailer et al., 2007; Trentacoste et al., 2012).

57 In olive trees, oil synthesis takes place mainly in the parenchymatic cells of the fruit
58 mesocarp (Rapoport and Moreno-Alías, 2017), but it is not until pit hardening has been
59 completed that oil accumulation starts properly becoming the main sink for the assimilates
60 allocated to fruits (Beltrán et al., 2017; Rapoport et al., 2013; Rapoport et al., 2017).
61 Existing evidence suggest that the rate of oil accumulation is very high in late summer/early
62 autumn and then decreases until the fruit reaches physiological maturity (Beltrán et al.,
63 2005; García-Martos and Mancha, 1992; Trentacoste et al., 2010). However, both oil
64 accumulation rate and ripening duration are substantially affected by fruit load (Barone et
65 al., 1994; Dag et al., 2011, Fernández et al., 2015, 2018), cultivar characteristics
66 (Camposeo et al., 2013; Lavee and Wodner, 1991) and both environmental and
67 agronomical conditions (Gucci et al., 2019; Lazzez et al., 2011; Mailer et al., 2007). The
68 concurrent effects of these factors challenge the definition of simple rules for determining
69 the date at which fruits reach their maximum oil content.

70 Establishing rational criteria for deciding the best harvest date still represents a major
71 challenge due to the existence of several trade-offs acting simultaneously. On the one hand,
72 late harvests obviously ensure achieving high oil contents while simultaneously favor low
73 fruit detachment force (Beltrán et al., 2017; Gamli and Eker, 2017), which can be critical
74 for the harvesting operation for some cultivars. On the other hand, harvesting early prevents
75 yield losses associated to natural fruit abscission and leads to oils of higher quality due to
76 higher contents of some minor components that are responsible of some of the
77 nutraceutical, organoleptic and gastronomic attributes of olive oil, such as polyphenols and
78 tocopherols (Aguilera et al., 2017; Alagna et al., 2012; Caponio et al., 2001; Dag et al.,
79 2011). In fact, the increasing pressure for obtaining oils of the maximum quality is already
80 promoting an advance in the harvest date among the olive oil production sector.

81 In any case, farmers still lack simple inexpensive methods that allow them to decide the
82 harvest date with some rational basis. In the best case, oil concentration is determined from
83 fruit samples and compared to threshold values indicating on how far the orchard is from
84 exploiting its oil accumulation potential (Zipori et al., 2016). This information is used to
85 decide whether harvest should start or not. Obviously, recurrent olive samplings are
86 required during the autumn to have a clear idea on how oil accumulation develops, which
87 comes at an unaffordable cost for many farmers. The maturity index, based on fruit color
88 (Beltrán et al., 2017), has also been used as an orientating approach for the decision-making
89 of harvest timing, but the correlation between color and oil concentration is poor in many
90 genotypes (Mickelbart and James, 2003; Navas-Lopez et al., 2019). Many other
91 physiological and biochemical parameters such as fruit respiration (Ranalli et al., 1998),
92 fruit detachment force (Almeida et al., 2016; Camposeo et al., 2013), changes in oil
93 composition (Beltrán et al., 2017) and sugar content kinetics (Trapani et al., 2016) have

94 also been related to optimal harvesting periods, but they are more difficult to implement in
95 practice and still require further research to assess the robustness of their relationships with
96 oil concentration.

97 The aim of this article is to provide and test new simple approaches for predicting oil
98 content dynamics based on inexpensive measurements of fruit dry weight that could be
99 easily used by growers as a support for deciding the optimal harvest timing. Briefly, we
100 consider that, since the start of oil accumulation, fruit oil content, “ O_f ” (g oil fruit⁻¹), can be
101 linearly related to fruit dry weight “ w_f ” (g fruit⁻¹) as:

$$102 \quad O_f = \beta (w_f - w_{f0}) = \beta w_f - \beta w_{f0} \quad (1)$$

103 Where w_{f0} (g fruit⁻¹) is the fruit dry weight at the onset of oil accumulation (i.e. at the end
104 of pit hardening) and β (g oil g⁻¹) is the amount of oil accumulated per g of fruit dry weight
105 increase since the start of oil accumulation (Fig. 1). w_{f0} should depend on fruit growth rate
106 from bloom to the end of pit hardening and must be cultivar dependent. β may also be
107 cultivar-specific, but we hypothesize that it remains constant during the whole oil
108 accumulation period and that it is independent of any factor affecting the availability of
109 assimilates for fruit growth such as water status or crop load. This would imply that the oil
110 content of fruits increases proportionally to fruit dry weight from the end of pit hardening
111 to maturity, irrespective of the fact that fruit growth rates can vary with time or among trees
112 of the same cultivar subjected to different conditions. Under these assumptions, recurrent
113 measurements of w_f could be easily used for tracking O_f dynamics throughout the oil
114 accumulation period.

115 The specific goals of this study are: (i) to test in different olive cultivars that oil
116 accumulation represents a fixed fraction of fruit growth (i.e. constant β), evaluating likely
117 genotypic differences in this trait, (ii) to test whether β is independent of factors affecting

118 fruit growth rates, particularly, crop load and water status, and (iii) to propose and test
119 simple approaches derived from the conceptual model for predicting oil accumulation
120 dynamics based on inexpensive measurements of w_f , assessing its strengths and
121 weaknesses. A compilation of data on fruit dry weight and oil accumulation dynamics
122 coming from four experiments with young-potted and mature field-grown olive trees are
123 used to address these objectives.

124

125 **2. Materials and methods**

126 *2.1. Experiment I*

127 Experiment I was performed in 2017 with 2 years-old trees of five olive cultivars:
128 ‘Arbequina’, ‘Picual’, ‘Arbosana’, ‘Frantoio’ and ‘Changlot Real’ growing outdoors in 25-
129 L pots at the Institute for Sustainable Agriculture (IAS-CSIC, Córdoba, Spain, 37.8°N,
130 4.8°W, 90m altitude). The substrate of the pots was composed of a mixture of sand (30 %),
131 silt (15 %) and peat (55 %). Ten trees per cultivar were planted in the winter of 2016 and
132 maintained under appropriate growing conditions since then by applying drip-irrigation and
133 slow-release fertilizers. In particular, enough irrigation was supplied to cover the maximum
134 evapotranspiration. Water requirements were established from ad hoc periodical
135 measurements of 24-h weight loss of the tree pots. The main meteorological variables were
136 recorded throughout the experiment with an automated weather station located 500 m apart.
137 The climate in the area is typically Mediterranean, with 580 mm of average rainfall mainly
138 concentrated between autumn and spring, and 1390 mm of average reference
139 evapotranspiration (ET_0).

140 In 2017, four trees per cultivar were selected for the experimental measurements. Samples
141 of five fruits per tree were collected at different moments of the fruit growing cycle starting

142 on July 19th and finishing in December 15th. After collecting the samples, the fruits were
143 weighted for determining their fresh weight and, then, oven dried for 42 h at 105 °C to
144 obtain w_f . Their oil content was subsequently measured using a NMR oil analyser (Del Río
145 and Romero, 1999).

146

147 *2.2. Experiment II*

148 Experiment II was conducted through the years 2011, 2012 and 2013 within a 22.2-ha
149 commercial hedgerow olive (cv. ‘Arbequina’) orchard located in ‘La Harina’ farm (20 km
150 to the southeast of Córdoba, Spain, 37.7°N, 4.6°W, 170 m altitude). The orchard was
151 planted in 2005 with 4 × 1.5 m tree spacing over a soil of clayish texture classified as a
152 Vertisol (López-Bernal et al., 2015).

153 Four irrigation treatments were established using a randomized complete block
154 experimental design with four replicates. Each of the 16 plots consisted of 40 trees in four
155 adjacent rows. The irrigation treatments included a fully irrigated control (FI) that applied
156 enough water to satisfy the maximum ET assuming a maximum crop coefficient of 0.75.
157 The remaining treatments consisted of two similar regulated deficit irrigation treatments
158 (D1 and D2) differing in the timing of the imposed water deficit and in its severity (Table
159 S1), to which we added an additional treatment mimicking the irrigation applied by the
160 manager of the commercial orchard (MI). The annual amounts of applied irrigation are
161 shown for each treatment and year in Table 1, along with cumulative values of rainfall and
162 ET_0 . Monthly values of those variables are also presented in the Supplementary Material
163 (Table S1). Information on how the FI, MI and D2 irrigation treatments affected tree water
164 status, trunk growth, transpiration and assimilation is available in López-Bernal et al.

165 (2015). Crop load was high in 2011 and 2013, and low in 2012, irrespective of the
166 irrigation treatment (Table 1).

167 The time courses of w_f and O_f were periodically monitored every year from midsummer
168 (July-August) to the orchard harvest date (late November-early December) in randomly
169 hand-picked samples of 72 fruits per irrigation treatment and block. Fruits were always
170 taken from the six central trees of the plots (12 fruits per tree). Fresh and dry weight of
171 fruits and their oil content were measured as in Experiment I.

172

173 *2.3. Experiment III*

174 Measurements were performed in 2014 in a 12-year old organic commercial olive (cv.
175 ‘Cobrançosa’) orchard located at “Vilariça” Valley (Trás-os-Montes, Portugal, 41.3 °N, 7.0
176 °W, 150 m altitude), a typical olive growing area of Northeast Portugal. The climate in the
177 area is Mediterranean (IPMA, 2015), with an average rainfall of 520 mm concentrated from
178 autumn to spring, and 1130 mm of average ET_0 . The soil is classified as Eutric Leptosols
179 developed on metamorphic rocks (schists), of sandy loam texture. Tree spacing was 7 x 7 m
180 and the experimental design was a complete randomized block, replicated three times. Each
181 plot contained four central olive trees surrounded by 14 border trees and all measurements
182 were made on the central trees of each plot.

183 Since 2013, five irrigation treatments were imposed in the orchard:

184 - FI: fully irrigated control, for which the water applied equaled the difference between the
185 maximum (estimated) ET and rainfall.

186 - PRD: partial root drying system applying the same irrigation dose as FI to one half of the
187 root system, with the irrigated and drying halves of the root-zone alternating every two
188 weeks.

189 - SD40: sustained deficit irrigation that regularly received 40% of the water applied to FI
190 - RD75: regulated deficit irrigation that received 75% of the water applied to FI, with a
191 midsummer deficit period from mid-July to mid-August, reducing irrigation to 15% of FI.
192 - RD40: regulated deficit irrigation that received the same seasonal amount of irrigation as
193 SD40 with a midsummer deficit period without irrigation from mid-July to mid-August.
194 Measurements of w_f and O_f were performed for each treatment at three different dates in
195 2014 (October 2nd, October 20th and November 12th), using samples of 40 fruits per tree
196 (three trees per treatment). That year crop load was low with no noticeable differences
197 among irrigation treatments. Determinations of oil content were based on Soxhlet
198 extraction (Donaire et al., 1977).

199

200 *2.4. Experiment IV*

201 Experiment IV was conducted in a 10-year old commercial olive (cv. ‘Cobrançosa’)
202 orchard located at Vilarica Valley (Trás-os-Montes, Portugal, 41.3 °N, 7.0 °W, 240 m
203 altitude), in the same area as the previous experiment. The soil is classified as Eutric
204 Leptosols developed on metamorphic rocks (schists), of sandy loam texture. Tree spacing
205 was 6 x 6 m. The design of the experimental plot consisted of three adjacent blocks, each of
206 these made of four rows with twenty olives trees, where only the six central trees were used
207 for sampling. Three irrigation treatments were imposed during three consecutive seasons
208 starting in 2004: full irrigation (FI), that received a seasonal water equivalent to 100%
209 estimated crop evapotranspiration; sustained deficit irrigation (SD30), that received a
210 volume of water equivalent to 30% of FI; and a rainfed treatment (RF).

211 In 2006, samples of 40 fruits per tree in 4 trees per treatment were collected periodically
212 from September to December to monitor the dynamics of w_f and O_f . The latter was

213 determined by Soxhlet extraction. That year crop load was the highest of the three
214 experimental seasons, with FI and RF showing the highest and lowest fruit numbers,
215 respectively (Fernandes-Silva et al., 2010).

216 Further information describing the orchard characteristics, the climatic conditions during
217 the experiment, the irrigation amounts applied to each treatment and their impacts on the
218 water status and productivity of the trees is provided in Fernandes-Silva et al. (2010).

219

220 *2.5. Hypothesis testing*

221 Linear regression analyses of O_f versus w_f were performed to test whether β can be
222 assumed both constant during the ripening period (i) and independent of the carbon
223 availability for fruit growth (ii). As these assumptions refer to the oil accumulation phase
224 only, data with oil concentrations below 5 % on a dry matter basis were, whenever present,
225 excluded from the analyses. According to the conceptual model (Eqn. 1), β was estimated
226 from the slope of the linear fit and w_{f0} was deduced from the intercept (as it should equal
227 the product of β and w_{f0}).

228 In Experiment I, regressions were performed for each cultivar independently, allowing us to
229 compare the differences in the resulting linear models. Water stress and crop load
230 presumably affect the availability of assimilates for fruit growth, so separate regressions
231 were conducted for each irrigation treatment in Experiments III and IV, and for each
232 combination of “irrigation treatment” x “year” in Experiment II. Finally, the regression
233 lines were compared experiment by experiment, evaluating the statistical significance of the
234 differences in the slopes and intercepts among the linear fits with the software Statistix 10
235 for Windows (Analytical Software, Tallahassee, FL, USA).

236 An additional quantitative assessment of the sensitivity of model parameters to carbon
237 availability was performed in Experiment II. Estimates of tree assimilation (López-Bernal
238 et al., 2015) and records of crop load (Table 1) were used to calculate the cumulative values
239 of assimilation per fruit (A_f , g C fruit⁻¹) for periods preceding (June 18th to July 18th, A_{f1})
240 and following (August 2nd to September 26th, A_{f2}) the onset of the oil accumulation phase.
241 The dependency of w_{f0} and β on carbon availability was assessed from plots of their
242 apparent values (obtained from the linear fits) versus A_{f1} and A_{f2} , respectively. The choice
243 of the starting and ending dates of the two periods was constrained by both the availability
244 of assimilation records for the three years and the uncertainty regarding the timing of the
245 onset of oil accumulation. We left a gap between the two periods on purpose because,
246 under the conditions of Southern Spain, the start of the oil accumulation phase has been
247 reported to start 10-12 weeks after full bloom (Beltrán et al., 2017; García and Mancha,
248 1992), with the average flowering date for ‘Arbequina’ in Córdoba being May 10th (De
249 Melo-Abreu et al., 2004) (unfortunately, the actual dates of full bloom were not recorded in
250 Experiment II).

251

252 *2.6. Testing model's predictive power in practice*

253 If the conceptual model presented in Eqn. 1 is sound in practice, then oil accumulation
254 dynamics could be easily predicted from routinely measurements of w_f . Any increase in w_f
255 over time can be translated into an increase in O_f by multiplying by β . Furthermore,
256 absolute values of O_f can also be theoretically estimated if a) oil concentration is measured
257 once on a representative sample of fruits at any time during the oil accumulation phase or,
258 b) if w_f is sampled around the date at which the oil accumulation phase starts in midsummer

259 (when $w_f = w_{f0}$). These two simple approaches (hereafter referred as ‘Approach A’ or
260 ‘Approach B’) were tested for the cultivar ‘Arbequina’.

261 The dataset of Experiment I was used for calibrating the value of β , while that of
262 Experiment II was selected for validation. In Approach A, the intercept of the model (O_{f0})
263 is calibrated, for each combination of “irrigation treatment” x “year”, as:

$$264 \quad O_{f0} = O_{fj} - \beta w_{fj} \quad (2)$$

265 where w_{fj} and O_{fj} are the average dry weight and oil content of a representative sample of
266 fruits taken on day ‘j’. For testing purposes, O_{f0} was calculated from the measured values of
267 w_{fj} and O_{fj} that were the closest to October 1st each year (‘j’ was October 5th in 2011,
268 October 1st in 2012 and September 24th in 2013).

269 In Approach B, O_{f0} was determined from the product of β and w_{f0} , the latter estimated for
270 each combination of “irrigation treatment” x “year” from the time course of w_f , assuming
271 three fixed-date scenarios for the onset of the oil accumulation phase: July 20th, August 1st
272 and August 10th. We selected these dates due to the aforementioned uncertainty regarding
273 the onset of oil accumulation.

274 Model performances in reproducing measured oil dynamics were assessed using mean
275 absolute error (MAE; from 0 to $+\infty$, optimum 0), root mean square error (RMSE; from 0 to
276 $+\infty$, optimum 0) and coefficient of residual mass (CRM, from $-\infty$ to $+\infty$, optimum 0):

$$277 \quad MAE = \sum_i^n |S_i - M_i|/n \quad (3)$$

$$278 \quad RMSE = \sqrt{\sum_i^n (S_i - M_i)^2/n} \quad (4)$$

$$279 \quad CRM = 1 - \sum_i^n S_i / \sum_i^n M_i \quad (5)$$

280 Where M_i is the i th measured oil, S_i is the i th simulated oil and n is the number of O_f
281 measurements.

282

283 **3. Results**

284 *3.1. Model's proof of concept*

285 The linear regression fits performed for each and every independent dataset of $O_f - w_f$ were
286 always highly significant ($P < 0.001$), with the determination coefficient ranging from 0.72
287 (Experiment IV, FI) to 0.999 (Experiment II, MI in 2013) and averaging 0.940 (Table 2).

288

289 *3.2. Carbon availability effects*

290 The time courses of w_f and O_f in Experiment II (cv. 'Arbequina') exhibited considerable
291 differences among years and irrigation treatments (Figure 2). On the one hand, the year of
292 low crop load (2012, Table 1) always led to fruits of higher weight and oil content than its
293 high crop load counterparts. On the other, FI showed higher values of w_f and O_f in 2012
294 and 2013 than D1 and D2, although slight differences were noticed among treatments in
295 2011. MI presented similar patterns of w_f and O_f to those of FI in 2011 and 2012, but it was
296 the treatment with the lowest values in 2013. These differences in the patterns of fruit
297 growth and oil accumulation among treatments were in consonance with the differences in
298 water status and assimilation rates reported by López-Bernal et al. (2015) in the same
299 experiment. In any case, estimates of A_f revealed that inter-annual differences in crop load
300 had a higher weight on the carbon availability per fruit than the differences in water status
301 among treatments (Fig. 3).

302 The values of β , estimated as the slope of the linear fits of O_f versus w_f , averaged 0.79 g oil
303 g^{-1} and ranged from 0.70 to 0.87 g oil g^{-1} (Table 2). All treatments averaged similar β , and
304 no significant differences among them were found when they were compared within each
305 year (Table S2). By contrast, the tests revealed statistically lower β for 2013 in relation to

306 2011 and 2012 in most cases (Table S2) and a slight direct relationship was found between
307 this parameter and A_{f2} (Fig. 3A). The slope resulting from the linear regression between β
308 and A_{f2} was significant ($P < 0.02$), although its value was low. No single combination of
309 “irrigation treatment” x “year” showed significant differences in β in relation to the value
310 obtained in Experiment I for the same cultivar (Table 2).

311 The intercept of the set-specific linear fits ranged from -0.34 to -0.15 g oil fruit⁻¹ (average -
312 0.25 g oil fruit⁻¹) (Table 2). Significant differences were usually found when comparing the
313 same treatment among years and when comparing the treatments in each year, except for
314 2011 (Table S2). The high variability in the intercepts was mainly driven by large
315 differences in w_{f0} . In this regard, its apparent values ranged from 0.21 to 0.39 g fruit⁻¹
316 (Table 2, average 0.31 g fruit⁻¹). The highest w_{f0} were observed in the low crop load year
317 (irrespective of the treatment), and deficit irrigation treatments resulted in lower values than
318 FI in 2012 and 2013. Moreover, the apparent estimates of w_{f0} presented a robust correlation
319 with A_{f1} ($r^2 = 0.84$, $P < 0.001$, Fig. 3B).

320 ‘Cobrançosa’ datasets generally showed no statistical differences when the slope or the
321 intercept of the linear fits were compared among either irrigation treatments or experiments
322 (Table S3, Fig. 4). Even if non-significant, differences in the estimates of w_{f0} between
323 experiments were considerable, averaging 0.33 g fruit⁻¹ in Experiment III and 0.57 g fruit⁻¹
324 in Experiment IV (Table 2). Slightly higher values of β were also found in Experiment IV,
325 irrespective of the treatment. In the FI treatments, β yielded 0.49 g oil g⁻¹ in Experiment III
326 and 0.62 g oil g⁻¹ in Experiment IV.

327

328 *3.3. Cultivar effects*

329 No statistical differences were found among cultivars for β in Experiment I (Table S4), its
330 values ranging from 0.75 ('Arbequina') to 0.82 ('Arbosana') g oil g⁻¹ (Table 2). The linear
331 fits of O_f versus w_f were parallels, evidencing clear differences in their intercepts (Fig. 5,
332 Table S4). In this regard, w_{f0} ranged from 0.26 ('Arbosana') to 0.60 ('Picual') g fruit⁻¹.
333 With the exception of the treatments FI and SD30 in Experiment IV, the slope of the fits
334 obtained for 'Cobrançosa' was always significantly lower than those observed for the five
335 cultivars tested in Experiment I (Fig. 5, Table 2).

336

337 *3.4. Performance of Approach A in predicting oil accumulation dynamics*

338 Using the dataset of Experiment I for calibrating the slope of the model for 'Arbequina' led
339 to $\beta = 0.75$ g oil g⁻¹ (Table 1). As the intercept of the model is considered to be affected by
340 carbon availability per fruit, it was obtained from pair measurements of w and oil around
341 October 1st for each set in Experiment II (Eqn. 2). Its values were the lowest in 2012 and
342 the highest in 2013, ranging from -0.28 to -0.17 g oil fruit⁻¹.

343 Using the routine measurements of w_f during the oil accumulation phase to feed the model,
344 O_f predictions agreed very closely with observations irrespective of the year and irrigation
345 treatment, as shown by the vicinity of the plots to the 1:1 line in Fig. 6. The satisfactory
346 performance of Approach A for reproducing O_f dynamics is also supported by the low
347 values of MAE (0.008 g oil fruit⁻¹), RMSE (0.013 g oil fruit⁻¹) and CRM (0.01), the latter
348 indicating a negligible bias.

349

350 *3.5. Performance of Approach B in predicting oil accumulation dynamics*

351 In Approach B, the model intercept is calibrated from the product of the slope (0.75 g oil g⁻¹
352 ¹, obtained from the independent set of 'Arbequina' in Experiment I) and w_{f0} , the latter

353 being estimated for three hypothetical date scenarios for the start of the oil accumulation
354 phase. Using this procedure, the intercept averaged -0.21, -0.24 and -0.26 g oil fruit⁻¹ for
355 the date scenarios July 20th, August 1st and August 10th, respectively. Regardless of the date
356 scenario, the intercepts were always the lowest in 2012 and the highest in 2013.

357 Model performance was the best in overall terms assuming August 1st as the date for the
358 onset of oil accumulation, with MAE, RMSE and CRM being 0.021 g oil fruit⁻¹, 0.027 g oil
359 fruit⁻¹ and 0.09, respectively (Table 3). However, the best date scenario was different when
360 each year was analyzed independently. For instance, the model made the best predictions of
361 oil for the year 2011 under the date scenario of July 20th, while August the 10th was the best
362 for reproducing oil accumulation dynamics in the year 2013 (Fig. 7).

363

364 **4. Discussion**

365 This study presents a simple conceptual model in which oil accumulation is linearly related
366 to fruit growth on a dry matter basis. The two model parameters can be associated with
367 physiologically relevant traits: the slope (β) is the fraction of dry weight growth that
368 accumulates in the fruit as oil, while the intercept is given by the product of β and fruit dry
369 weight at the start of the oil accumulation phase (w_{f0}). All the plots of O_f versus w_f
370 compiled in the four experiments of this article exhibited satisfactory linear fits ($P < 0.001$)
371 with high determination coefficients (Table 2), which demonstrates the applicability of the
372 model.

373 Understanding the factors that affect model parameters is a pivotal step to assess how it can
374 be used in practice for predicting oil accumulation dynamics. In Experiment II
375 ('Arbequina'), β was significantly lower in 2013 than in 2011 and 2012 in most cases
376 (Table S2). This result might have been related with a lower assimilate availability per fruit

377 in 2013 (Fig. 3), contrary to our starting hypothesis, but the likely effect of carbon
378 availability on β is of limited importance actually (or at least it was so for the range of A_f
379 covered in Experiment II). This is evidenced by the excellent performance of Approach A
380 in reproducing oil accumulation dynamics for all the independent datasets (Fig. 6, Table 3)
381 even if a fixed and independent value of β was always used. The lack of statistical
382 differences among irrigation treatments in Experiments III and IV also support the premise
383 of a negligible effect of carbon availability on β for ‘Cobrançosa’ (Fig. 4, Table S3). We
384 must acknowledge, however, that assessing differences in A_f among treatments or
385 experiments in those datasets was not possible with the available experimental information.
386 Despite slight and non-significant differences among cultivars being noticed in Experiment
387 I, the values of β obtained for ‘Cobrançosa’ in Experiments III and IV revealed
388 substantially lower values. Consequently, β might be genotypically controlled, which
389 would imply that this parameter requires cultivar-specific calibration.

390 Significant cultivar variability was also observed for w_{f0} in Experiment I, which was
391 somehow expected as differences in fruit size among cultivars are usually evident from a
392 few weeks after flowering (Beltrán et al., 2017; Lavee and Wodner, 1991). This fact
393 originates, mainly, from genotypic differences in the rates of cell division (Hammami et al.,
394 2011). Besides cultivar variability, w_{f0} also seems to be significantly determined by carbon
395 availability as evidenced by results in Experiment II, where high crop load and water
396 deficits led to lower values (Fig. 3, Table 2). Both the high rates of cell division and
397 expansion in the first weeks following flowering and the production of lignin during pit
398 hardening are metabolically expensive processes (Hammami et al., 2011, 2013; Rapoport et
399 al., 2017), which explains why any limitation in the availability of assimilates is expected

400 to reduce w_{f0} . As a corollary, w_{f0} can vary every season even for the same orchard and
401 cultivar, so it is a parameter that requires both year- and orchard-specific calibration.

402 Two approaches for calibrating w_{f0} are implicitly proposed in this paper assuming that β is
403 both independent of carbon availability and genotypically-controlled. If the cultivar-
404 specific value of β is available, the first approach (Approach A) just requires a single
405 measurement of w_f and O_f from a representative fruit sample at any time during the oil
406 accumulation phase to calibrate w_{f0} . The second (Approach B) prevents the need for oil
407 determinations requiring, instead, measuring w_f at the date at which the oil accumulation
408 phase begins. Both approaches can potentially yield excellent results, as demonstrated by
409 the model performance tests conducted for Experiment II (Table 3, Fig. 6, Fig. 7).
410 However, it must be noted that choosing the date of the onset of oil accumulation is rather
411 challenging, as it varies from year to year, which translates into substantial bias in
412 subsequent model predictions (Fig. 7, Table 3). The economic advantage of Approach B
413 (no single O_f determination is needed) comes, therefore, at the cost of limited reliability in
414 relation to Approach A when an absolute estimate of O_f is required. Nevertheless, we must
415 note also that both approaches will yield equally reliable estimates of the rate of oil
416 accumulation in the period between consecutive measurements of w_f .

417 The development of simple methods to predict the onset of oil accumulation seems a
418 desirable target for future research. So far, measurements of pit breaking resistance with
419 penetrometer devices (Rapoport et al., 2013) might provide a good indication of the ideal
420 date for measuring w_{f0} , as oil accumulation is likely to start when pit hardening (and its
421 competition for assimilates against the mesocarp) is reaching an end (Beltrán et al., 2017;
422 Rapoport et al., 2017), but such measurements might be too laborious to be applied by
423 farmers. On the other hand, a simple model for predicting the onset of oil accumulation

424 based on thermal time has been proposed for several cultivars in the arid environment of
425 Mendoza, Argentina (Trentacoste et al., 2012). Unfortunately, the model has not been
426 validated in the Mediterranean area and remains empirical, as acknowledged by their
427 developers. In this regard, a simple thermal time approach might not be entirely satisfactory
428 for predicting the onset of oil accumulation, as there are evidences pointing that the
429 duration of pit hardening is affected by water stress (Hammami et al., 2013).

430 Beyond detailed technical examinations of parameter calibration, the model presented in
431 this study is of the greatest relevance for the olive growing sector, as most farmers still lack
432 inexpensive methods for following oil accumulation dynamics and rational criteria to
433 decide the most appropriate harvest date accordingly. The best approach for monitoring oil
434 accumulation dynamics to date depends on periodical determinations of oil concentration,
435 which can be expensive for small growers. Our results suggest that recurrent measurements
436 of w_f might be enough to predict oil accumulation dynamics reducing the number of
437 determinations of oil concentration to a minimum (i.e. to “one” single determination if
438 Approach A is used). Moreover, even if oil concentration cannot be determined, the model
439 is able to predict oil accumulation rates (any increase in w_f can be easily converted into O_f
440 multiplying by β) and theoretically yields approximate estimates of O_f if w_f is measured
441 around the date at which the oil accumulation starts (Approach B). Another implicit point
442 in our conceptual model is that the growth of w_f should stop once the fruit reaches its
443 maximum O_f . From the practical point of view, this implies that the maximum oil content
444 could be determined when w_f reaches a plateau. However, we must acknowledge that the
445 absence of late harvests in our experiments prevented us to probe that point thoroughly.

446 Despite our results being promising, the conceptual model and its derived practical
447 applications require further testing under contrasting environmental and agronomical

448 conditions including different cultivars in order to better assess their reliability. In this
449 regard, many studies report that oil accumulation rates decrease under high temperatures
450 (Lavee et al., 2012; García-Inza et al., 2014; Rondanini et al., 2014; Benlloch-González et
451 al., 2019; Nissim et al., 2020). These observations might suggest that β is reduced at high
452 temperatures, but the evidences available are not fully conclusive because the reduced oil
453 accumulation rates may as well be the result of a decrease in fruit dry weight accumulation.
454 In any case, we are confident that many researchers could easily contribute to the testing of
455 the model under contrasting temperatures, environments or agronomical management
456 conditions using already collected datasets of w_f and O_f . Finally, the model may also be
457 used within a process-based model of olive orchards like OliveCan, which currently lacks a
458 mechanistic simulation of oil production (López-Bernal et al., 2018).

459

460 **5. Conclusion**

461 This paper presents a conceptual model that estimates the oil content of olive fruits (O_f) as a
462 fixed proportion (β) of their dry weight increase since the onset of the oil accumulation
463 phase ($w_f - w_{f0}$). A compilation of datasets of paired oil content and weight determinations
464 from experiments with different cultivars and conditions of water status and crop load
465 supports the validity of the model. The two parameters of the conceptual model (β and w_{f0})
466 are physiologically-relevant traits and can be obtained from the slope and intercept of linear
467 regressions of O_f on w_f . Our results indicate that β could be cultivar-specific but remains
468 fairly unaffected by factors modulating the availability of carbon per fruit, such as crop
469 load or water stress. On the contrary, the fruit dry weight at the onset of oil accumulation
470 (w_{f0}) is both genotypically-controlled and dependent on crop load and photosynthesis
471 during the earlier stages of fruit growth, which implies that it requires orchard- and year-

472 specific calibration. Fortunately, the model allows for easily determining w_{f0} from a single
473 determination of O_f and w_f at any date during the oil accumulation phase provided that a
474 cultivar-specific value of β is available (Approach A), or, alternatively, it can be measured
475 directly if the date of the onset of oil accumulation can be estimated (Approach B). Overall,
476 these model features indicate that oil accumulation rates could be estimated reliably from
477 inexpensive measurements of w_f during autumn. This opens the door for providing olive
478 growers with simple affordable methods to estimate O_f , which is a critical indicator for
479 establishing optimal harvesting periods. Prior to that, further research testing the validity of
480 our findings for different environmental conditions and/or new cultivars would be highly
481 desirable.

482

483 **Acknowledgements**

484 This work was supported by the Spanish Ministry of Economy and Competitiveness
485 [project AGL-2015-69822] and also by National Funds by FCT - Portuguese Foundation
486 for Science and Technology [project UIDB/04033/2020]. The former project provided the
487 funding for setting up Experiment I. Experiment II was performed under the framework of
488 a project [P10-AGR-6456] funded by the Andalusian Regional Government. Experiment III
489 was supported by the PRODER program of the Portuguese Ministry of Agriculture [project
490 PA-44662-IF0019]. Experiment IV was funded by the AGRO-INIA program of the
491 Portuguese Ministry of Agriculture [project AGRO175] and by the PhD fellowship
492 [SFRH/BD/18441/2004] awarded to AF-S by the Foundation for Science and Technology
493 of the Portuguese Ministry of Science, Technology and Education. AL-B enjoyed a JAE-
494 Pre PhD scholarship during Experiment II (funded by CSIC) and a ‘Juan de la Cierva-
495 Formación’ postdoctoral fellowship (funded by the Spanish Ministry of Economy and

496 Competitiveness, grant number [FJCI-2015-24109]) during the execution of Experiment I.
497 We gratefully acknowledge the contribution of Dr. Francisco Orgaz in designing
498 Experiment II and the excellent assistance by Estrella Muñoz, Marcos Orgaz and José Luis
499 Vázquez in Experiment I.

500

501 **References**

502 Aguilera, M.P., Uceda, M., Beltrán, G., (2017) La calidad del aceite de oliva, in: Barranco,
503 D., Fernández-Escobar, R., Rallo, L. (Eds.), El cultivo del olivo. Mundi-Prensa,
504 Madrid, Spain, pp.839-868.

505 Alagna, F., Mariotti, R., Panara, F., Caporali, S., Urbani, S., Veneziani, G., Esposito, S.,
506 Taticchi, A., Rosati, A., Rao, R., Perrotta, G., Servili, M., Baldoni, L., 2012. Olive
507 phenolic compounds: metabolic and transcriptional profiling during fruit
508 development. BMC Plant Biol. 12, 162. <https://doi.org/10.1186/1471-2229-12-162>.

509 Almeida, A., Figueiredo, T., Fernandes-Silva, A., 2016. Evolution of factors affecting
510 mechanical olive harvesting. Acta Hort. 1139, 575-579.
511 <https://doi.org/10.17660/ActaHortic.2016.1139.99>.

512 Barone, E, Gullo, G., Zappia, R., Inglese, P., 1994. Effect of crop load on fruit ripening and
513 olive oil (*Olea europaea* L.) quality. J. Hort. Sci. 69, 67-73.
514 <https://doi.org/10.1080/14620316.1994.11515250>.

515 Beltrán, G., Aguilera, M.P., Del Río, C., Sánchez, S., Martínez, L., 2005. Influence of fruit
516 ripening process on the natural antioxidant content of Hojiblanca virgin olive oils.
517 Food Chem. 89, 207-215. <https://doi.org/10.1016/j.foodchem.2004.02.027>.

518 Beltrán, G., Uceda, M., Hermoso, M., Frías, L., (2017) Maduración, in: Barranco, D.,
519 Fernández-Escobar, R., Rallo, L. (Eds.), El cultivo del olivo. Mundi-Prensa, Madrid,
520 Spain, pp.187-212.

521 Benlloch-González, M., Sánchez-Lucas, R., Bejaoui, M.A., Benlloch, M., Fernández-
522 Escobar, R., 2019. Global warming effects on yield and fruit maturation of olive trees
523 growing under field conditions. *Sci. Hortic.* 249, 162-167.
524 <https://doi.org/10.1016/j.scienta.2019.01.046>.

525 Camposeo, S., Vivaldi, G.A., Gattullo, C.E., 2013. Ripening indices and harvesting times
526 of different olive cultivars for continuous harvest. *Sci. Hortic.* 151, 1-10.
527 <https://doi.org/10.1016/j.scienta.2012.12.019>.

528 Caponio, F., Gomes, T., Pasqualone, A., 2001. Phenolic compounds in virgin olive oils:
529 influence of the degree of olive ripeness on organoleptic characteristics and shelf-life.
530 *Eur. Food Res. Technol.* 212, 329-333. <https://doi.org/10.1007/s002170000268>.

531 Dag, A., Kerem, Z., Yogev, N., Zipori, I., Lavee, S., Ben-David, E., 2011. Influence of time
532 of harvest and maturity index on olive oil yield and quality. *Sci. Hortic.* 127, 358-
533 366. <https://doi.org/10.1016/j.scienta.2010.11.008>.

534 Del Río, C., Romero, A.M., 1999. Whole, unmilled olives can be used to determine their
535 oil content by nuclear magnetic resonance. *HortTechnology* 9, 675-680.
536 <https://doi.org/10.21273/HORTTECH.9.4.675>.

537 Donaire, J., Sanchez-Raya, A.J., Lopez-George, J.L., Recalde, L., 1977. Etudes
538 physiologiques et biochimiques de l'olivier: I. variation de la concentration de divers
539 metabolites pendant son cycle evolutif. *Agrochim.* 21, 311-321.

540 FAOSTAT, 2017. <http://www.fao.org/faostat/en/#data> (accessed 20 May 2020)

541 Fernandes-Silva, A.A., Ferreira, T.C., Correia, C.M., Malheiro, A.C., Villalobos, F.J.,
542 2010. Influence of different irrigation regimes on crop yield and water use efficiency
543 of olive. *Plant Soil* 333, 35-47. <https://doi.org/10.1007/s11104-010-0294-5>.

544 Fernández, F.J., Ladux, J.L., Hammami, S.B.M., Rapoport, H.F., Searles, P.S., 2018. Fruit,
545 mesocarp and endocarp responses to crop load and to different estimates of source:
546 sink ratio in olive (cv. Arauco) at final harvest. *Sci. Hortic.* 234, 49-57.
547 <https://doi.org/10.1016/j.scienta.2018.02.016>.

548 Fernández, F.J., Ladux, J.L., Searles, P.S., 2015. Dynamics of shoot and fruit growth
549 following fruit thinning in olive trees: same season and subsequent season responses.
550 *Sci. Hortic.* 192, 320-330. <https://doi.org/10.1016/j.scienta.2015.06.028>.

551 Gamli, Ö.F., Eker, T., 2017. Determination of harvest time of Gemlik olive cultivars by
552 using physical and chemical properties. *J. Food Meas. Charact.* 11, 2022–2030.
553 <https://doi.org/10.1007/s11694-017-9585-3>.

554 García-Inza, G.P., Castro, D.N, Hall, A.J., Rousseaux, M.C., 2014. Responses to
555 temperature of fruit dry weight, oil concentration, and oil fatty acid composition in
556 olive (*Olea europaea* L. Var. 'arauco'). *Eur. J. Agron.* 54, 107-115.
557 <https://doi.org/10.1016/j.eja.2013.12.005>.

558 García-Martos, J.M., Mancha, M., 1992. Evolución de la biosíntesis de lípidos durante la
559 maduración de las variedades de aceituna ‘Picual’ y ‘Gordal’. *Grasas y Aceites* 43,
560 277-280.

561 Gucci, R., Carusso, G., Gennai, C., Esposito, S., Urbani, S., Servili, M., 2019. Fruit growth,
562 yield and oil quality changes induced by deficit irrigation at different stages of olive
563 fruit development. *Agric. Water Manage.* 212, 88-98.
564 <https://doi.org/10.1016/j.agwat.2018.08.022>.

565 Hammami, S.B.M., Costagli, G., Rapoport, H.F., 2013. Cell and tissue dynamics of olive
566 endocarp sclerification vary according to water availability. *Physiol. Plantarum* 149,
567 571-582. <https://doi.org/10.1111/ppl.12097>.

568 Hammami, S.B.M., Manrique, T., Rapoport, H.F., 2011. Cultivar-based fruit size in olive
569 depends on different tissue and cellular processes throughout growth. *Sci. Hortic.*
570 130, 445-451. <https://doi.org/10.1016/j.scienta.2011.07.018>.

571 IPMA, 2015. <http://www.ipma.pt/pt/oclima/normais.clima/> (accessed 20 May 2020)

572 Lavee, S., Wodner, M., 1991. Factors affecting the nature of oil accumulation in fruit of
573 olive (*Olea europaea* L.) cultivars. *J. Hortic. Sci.* 66, 583-591.
574 <https://doi.org/10.1080/00221589.1991.11516187>.

575 Lavee, S., Haskal, A., Avidan, B., 2012. The effect of planting distances and tree shape on
576 yield and harvest efficiency of cv. Manzanillo table olives. *Sci. Hortic.* 142, 166-173.
577 <https://doi.org/10.1016/j.scienta.2012.05.010>.

578 Lazzez, A., Vichi, S., Kammoun, N.G., Arous, M.N., Khlif, M., Romero, A., Cossentini,
579 M., 2011. A four year study to determine the optimal harvesting period for Tunisian
580 Chemlali olives. Eur. J. Lipid Sci. Technol. 113, 796-807.
581 <https://doi.org/10.1002/ejlt.201000474>.

582 López-Bernal, Á., García-Tejera, O., Vega, V.A., Hidalgo, J.C., Testi, L., Orgaz, F.,
583 Villalobos, F.J., 2015. Using sap flow measurements to estimate net assimilation in
584 olive trees under different irrigation regimes. Irrig. Sci. 33, 357-366.
585 <https://doi.org/10.1007/s00271-015-0471-7>.

586 López-Bernal, Á., Morales, A., García-Tejera, O., Testi, L., Orgaz, F., De Melo-Abreu,
587 J.P., Villalobos, F.J., 2018. OliveCan: a process-based model of development, growth
588 and yield of olive orchards. Front. Plant Sci. 9, 632.
589 <https://doi.org/10.3389/fpls.2018.00632>.

590 Mailer, R.J., Ayton, J., Conlan, D., 2007. Influence of harvest timing on olive (*Olea*
591 *europaea*) oil accumulation and fruit characteristics under Australian conditions. J.
592 Food Agric. Environ. 5, 58-63.

593 Mickelbart, M.V., James, D., 2003. Development of a dry matter maturity index for olive
594 (*Olea europaea*). N. Z. J. Crop Hortic. Sci. 31, 269–276.
595 <https://doi.org/10.1080/01140671.2003.9514261>.

596 Navas-Lopez, J.F., León, L., Trentacoste, E.R., de la Rosa, R., 2019. Multi-environment
597 evaluation of oil accumulation pattern parameters in olive. Plant Physiol. Biochem.
598 139, 485-494. <https://doi.org/10.1016/j.plaphy.2019.04.016>.

599 Nissim, Y, Shloberg, M., Biton, I., Many, Y., Doron-Faigenboim, A., Zemach, H., Hovav,
600 R., Kerem, Z., Avidan, B., Ben-Ari, G., 2020. High temperature environment reduces
601 olive oil yield and quality. PLoS ONE 15, e0231956.
602 <https://doi.org/10.1371/journal.pone.0231956>.

603 Ranalli, A., Tombesi, A., Ferrante, M.L., De Mattia, G., 1998. Respiratory rate of olive
604 drupes during their ripening cycle and quality of oil extracted. J. Sci. Food Agric. 77,
605 359-367. [https://doi.org/10.1002/\(SICI\)1097-0010\(199807\)77:3<359::AID-
606 JSFA43>3.0.CO;2-R](https://doi.org/10.1002/(SICI)1097-0010(199807)77:3<359::AID-JSFA43>3.0.CO;2-R).

607 Rapoport, H.F., Hammami, S.B.M., Rosati, A., Gucci, R., 2017. Advances in olive fruit cell
608 and tissue development. Acta Hort. 1177.
609 <https://doi.org/10.17660/ActaHortic.2017.1177.29>.

610 Rapoport, H.F., Moreno-Alías, I., 2017. Botánica y morfología, in: Barranco, D.,
611 Fernández-Escobar, R., Rallo, L. (Eds.), El cultivo del olivo. Mundi-Prensa, Madrid,
612 Spain, pp.35-64.

613 Rapoport, H.F., Pérez-López, D., Hammami, S.B.M., Agüera, J., Moriana, A., 2013. Fruit
614 pit hardening: physical measurement during olive fruit growth. Ann. Appl. Biol. 163,
615 200-208. <https://doi.org/10.1111/aab.12046>.

616 Rondanini, D.P., Castro, D.N., Searles, P.S., Rousseaux, M.C., 2014. Contrasting patterns
617 of fatty acid composition and oil accumulation during fruit growth in several olive
618 varieties and locations in a non-Mediterranean region. Eur. J. Agron. 52, 237-246.
619 <https://doi.org/10.1016/j.eja.2013.09.002>.

620 Trapani, S., Migliorini, M., Cherubini, C., Cecchi, L., Canuti, V., Fia, G., Zanoni, B., 2016.
621 Direct quantitative indices for ripening of olive oil fruits to predict harvest time. Eur.
622 J.. Lipd Sci. Technol. 118, 1202-1212. <https://doi.org/10.1002/ejlt.201500317>.

623 Trentacoste, E.R., Puertas, C.M., Sadras, V.O., 2010. Effect of fruit load on oil yield
624 components and dynamics of fruit growth and oil accumulation in olive (*Olea*
625 *europaea* L.). Eur. J. Agron. 32, 249-254. <https://doi.org/10.1016/j.eja.2010.01.002>.

626 Trentacoste, E.R., Puertas, C.M., Sadras, V.O., 2012. Modelling the intraspecific variation
627 in the dynamics of fruit growth, oil, and water concentration in olive (*Olea europaea*
628 L.). Eur. J. Agron. 38, 83-93. <https://doi.org/10.1016/j.eja.2012.01.001>.

629 Zipori, I., Bustan, A., Kerem, Z., Dag, A., 2016. Olive paste oil content on a dry weight
630 basis (OPDW): an indicator for optimal harvesting time in modern olive orchards.
631 Grasas y Aceites, 67, e137. <https://doi.org/10.3989/gya.0764152>.

632

633 **Tables**

634 **Table 1.** Annual values of rainfall, reference evapotranspiration (ET₀) and applied
635 irrigation and fruit number for each irrigation treatment in Experiment II (FI, full irrigation;
636 MI, manager irrigation; D1, regulated deficit irrigation 1; D2, regulated deficit irrigation 2).

Year	Rain (mm)	ET ₀ (mm)	Applied irrigation (mm)				Fruit number (fruits m ⁻²)			
			FI	MI	D1	D2	FI	MI	D1	D2
2011	514	1229	465	326	306	243	859	745	779	772
2012	660	1266	591	376	471	240	307	391	387	406
2013	770	1178	536	144	277	219	1123	1116	1063	1055

637

638 **Table 2.** Results from independent linear regression analyses of fruit oil content (O_f , g fruit⁻¹) versus fruit dry weight (w_f , g fruit⁻¹) for each combination of “irrigation treatment” x
639 “year” x “cultivar” in the four experiments. Note that the slopes of the linear regression
640 lines are equivalent to β . The apparent dry weight at the start of oil accumulation (w_{f0}) is
641 calculated from the slopes and intercepts of linear fits. The last two columns ($P_{intercept}$ and
642 P_{slope}) show whether the slopes and intercepts differ statistically from the apparent value
643 obtained for the olive cultivar ‘Arbequina’ in Experiment I.

Experiment	Year	Cultivar	Treatment	n	Intercept (g fruit ⁻¹)	Slope (β) (g oil g ⁻¹)	r ²	w _{f0} (g)	P _{intercept}	P _{slope}
I	2017	Arbequina	FI	52	-0.22	0.75	0.88	0.29		
I	2017	Picual	FI	52	-0.48	0.80	0.80	0.60	***	n.s.
I	2017	Arbosana	FI	52	-0.21	0.82	0.92	0.26	***	n.s.
I	2017	Frantoio	FI	52	-0.33	0.74	0.96	0.45	***	n.s.
I	2017	Changlot	FI	52	-0.36	0.79	0.89	0.45	***	n.s.
II	2011	Arbequina	FI	5	-0.24	0.79	0.99	0.30	n.s.	n.s.
II	2011	Arbequina	MI	5	-0.26	0.84	1.00	0.31	n.s.	n.s.
II	2011	Arbequina	D1	5	-0.26	0.84	1.00	0.30	n.s.	n.s.
II	2011	Arbequina	D2	5	-0.26	0.84	1.00	0.31	n.s.	n.s.
II	2012	Arbequina	FI	7	-0.32	0.83	1.00	0.38	***	n.s.
II	2012	Arbequina	MI	7	-0.34	0.87	0.99	0.39	***	n.s.
II	2012	Arbequina	D1	7	-0.28	0.79	0.99	0.35	***	n.s.
II	2012	Arbequina	D2	7	-0.30	0.75	0.99	0.39	**	n.s.
II	2013	Arbequina	FI	8	-0.21	0.75	0.99	0.28	n.s.	n.s.
II	2013	Arbequina	MI	8	-0.15	0.72	1.00	0.21	***	n.s.
II	2013	Arbequina	D1	8	-0.18	0.72	1.00	0.25	n.s.	n.s.
II	2013	Arbequina	D2	8	-0.16	0.70	1.00	0.23	*	n.s.
III	2014	Cobrançosa	FI	9	-0.15	0.49	0.99	0.31	***	***
III	2014	Cobrançosa	PRD	9	-0.18	0.50	0.85	0.36	***	***
III	2014	Cobrançosa	RD75	9	-0.17	0.50	0.98	0.35	***	***

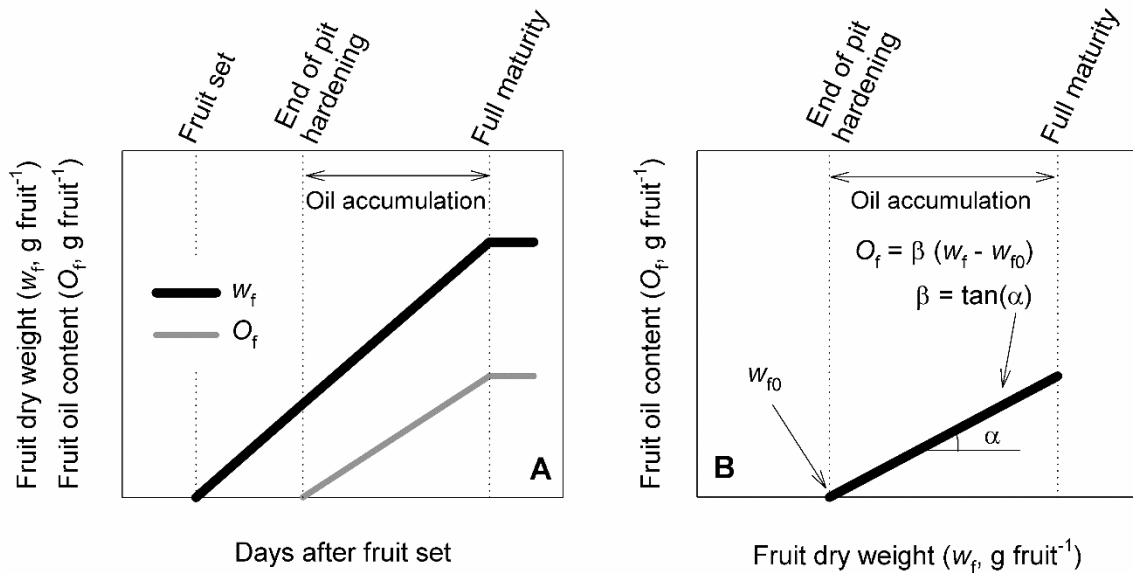
III	2014	Cobrançosa	RD40	9	-0.14	0.49	0.97	0.29	***	***
III	2014	Cobrançosa	SD40	9	-0.18	0.52	0.93	0.35	***	***
IV	2006	Cobrançosa	FI	20	-0.38	0.61	0.72	0.62	***	n.s.
IV	2006	Cobrançosa	SD30	20	-0.40	0.67	0.96	0.60	***	n.s.
IV	2006	Cobrançosa	RF	20	-0.28	0.57	0.91	0.49	***	**

646 **Table 3.** Performance of Approach A and Approach B (for three scenarios for the onset of
 647 oil accumulation) in reproducing fruit oil content (O_t) dynamics. MAE is mean absolute
 648 error, RMSE is root mean square error and CRM is coefficient of residual mass.

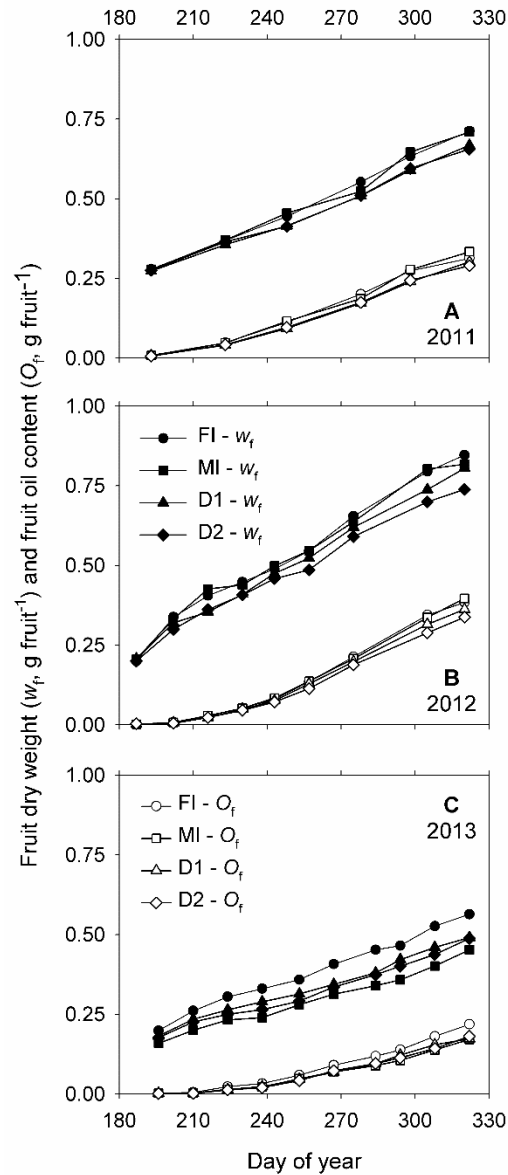
Parameter	Approach A	Approach B		
		July 20 th	August 1 st	August 10 th
n	80	80	80	80
MAE (g oil fruit ⁻¹)	0.008	0.027	0.021	0.032
RMSE (g oil fruit ⁻¹)	0.013	0.031	0.027	0.040
CRM	0.01	-0.15	0.09	0.23

649

650



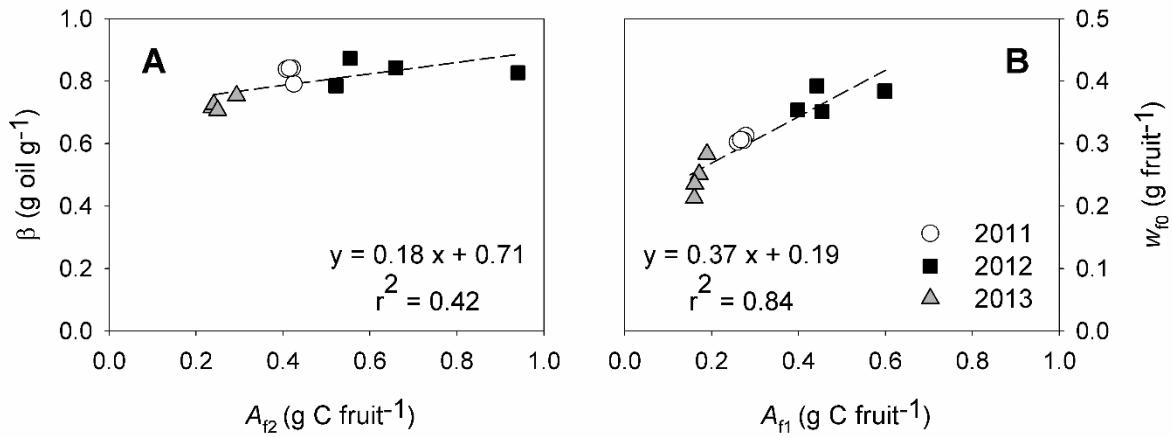
652
 653 **Fig. 1.** Graphical description of the main features of the conceptual model. Panel A shows a
 654 simplified time course of fruit dry weight (w_f) and oil content (O_f) from fruit set to full
 655 maturity. While the former increases throughout this period, oil accumulation only starts
 656 when the metabolically expensive pit hardening process has been completed. Panel B
 657 shows the plot of O_f versus w_f assuming that the amount of oil accumulated per unit of dry
 658 weight increase (β) is constant during oil accumulation. Under these conditions, O_f is
 659 linearly related to w_f from the end of pit hardening to full maturity. The slope of the $O_f - w_f$
 660 relationship during this period is indeed the parameter β while the intercept with the X-axis
 661 represents the fruit dry weight at the onset of oil accumulation (w_{f0}). Thus, both β and w_{f0}
 662 are physiologically relevant parameters that can be used to formulate a linear model to
 663 estimate O_f dynamics from those of w_f during the oil accumulation period.



665

666 **Fig. 2.** Time course of fruit dry weight (w_f , closed circles) and fruit oil content (O_f , open
 667 circles) in 2011 (A), 2012 (B) and 2013 (C) in Experiment II. Each type of symbol
 668 corresponds to a different irrigation treatment: circles, squares, triangles and diamonds for
 669 FI (full irrigation), MI (management irrigation), D1 (deficit irrigation 1) and D2 (deficit
 670 irrigation 2), respectively.

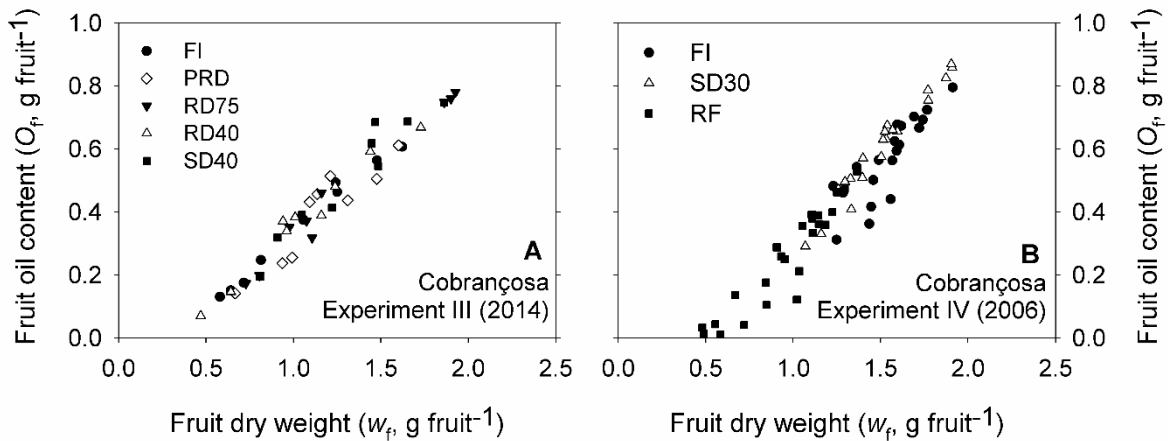
671



672

673 **Fig. 3.** Relationships between the fraction of fruit dry weight increase allocated to oil
 674 accumulation (β) and cumulative assimilation per fruit from August 2nd to September 26th
 675 (A_{f2} , A) and between fruit dry weight at the onset of oil accumulation (w_{f0}) and cumulative
 676 assimilation per fruit from June 18th to July 18th (A_{f1} , B). Data are grouped in years, (circles,
 677 squares and triangles for 2011, 2012 and 2013, respectively).

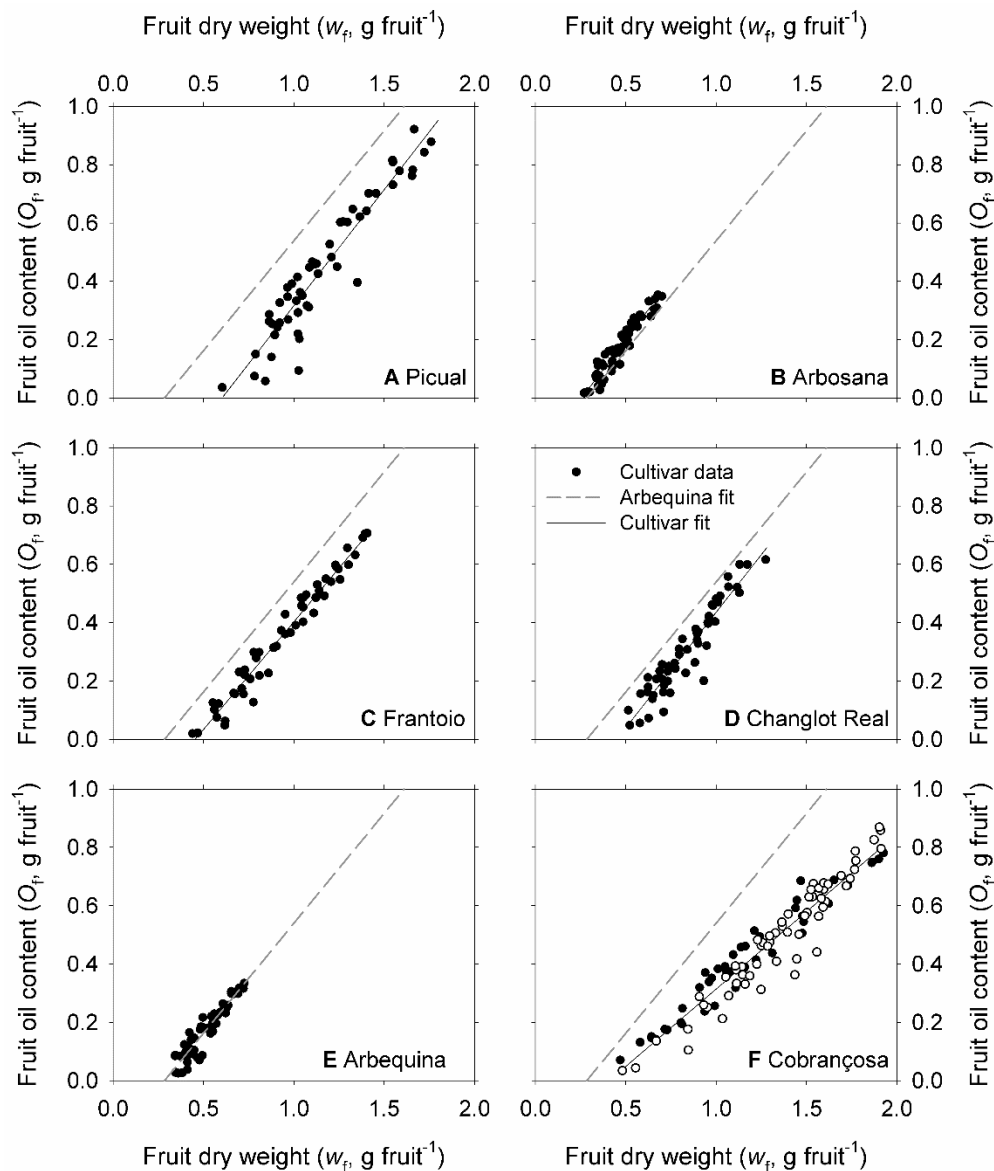
678



679

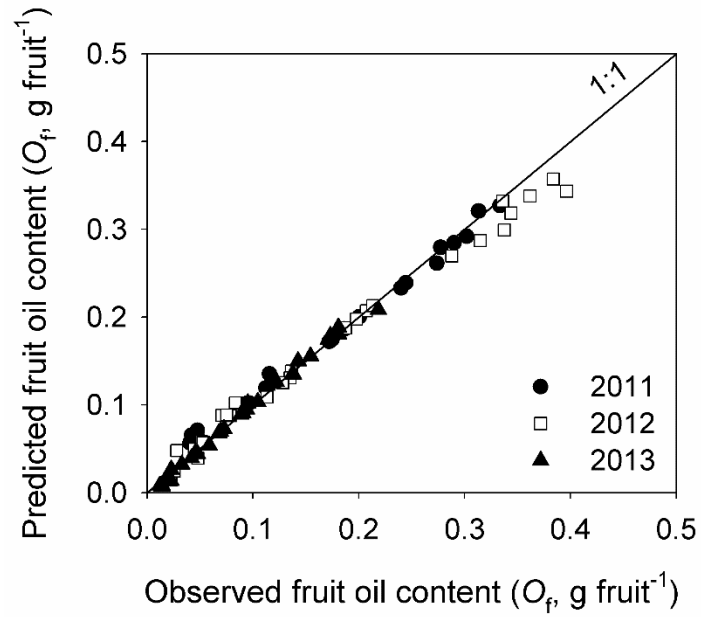
680 **Fig. 4.** Plots of fruit oil content (O_f) versus fruit dry weight (w_f) for the olive cultivar
 681 ‘Cobraçosa’ in Experiments III (A) and IV (B). Each type of symbol corresponds to a
 682 different irrigation treatment (FI, full irrigation; PRD, partial root drying; RD75, regulated
 683 deficit irrigation applying 75 % of FI; RD40, regulated deficit irrigation applying 40 % of
 684 FI; SD40, sustained deficit irrigation applying 40 % of FI; SD30, sustained deficit irrigation
 685 applying 30 % of FI; RF, rainfed).

686



687

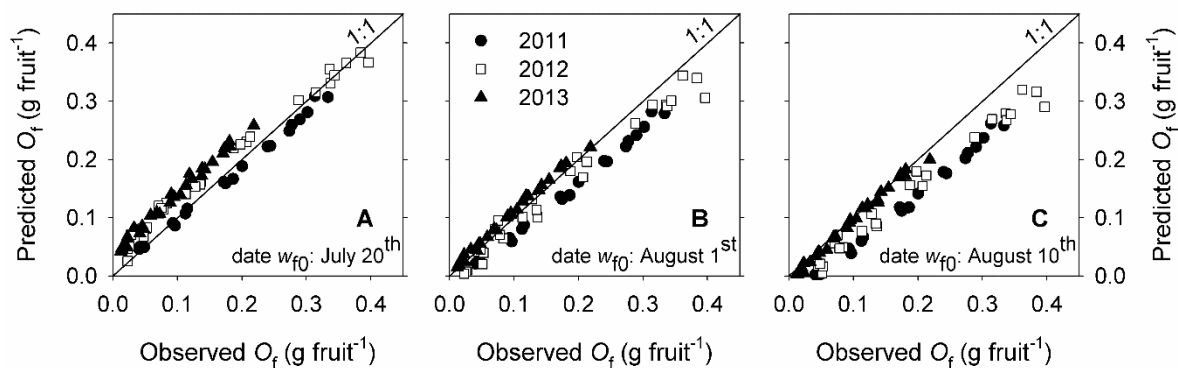
688 **Fig. 5.** Plots of fruit oil content (O_f) versus fruit dry weight (w_f) for the olive cultivars
 689 ‘Picual’ (A), ‘Arbosana’ (B), ‘Frantoio’ (C), ‘Changlot Real’ (D), ‘Arbequina’ (E) and
 690 ‘Cobrançosa’ (F). Data for ‘Picual’, ‘Arbosana’, ‘Frantoio’, ‘Changlot Real’ and
 691 ‘Arbequina’ come from Experiment I. Data for ‘Cobrançosa’ comes from Experiment III
 692 (closed symbols) and Experiment IV (open symbols), mixing all irrigation treatments. The
 693 linear fit obtained for ‘Arbequina’ in Experiment I is shown in all panels with a grey dashed
 694 line to serve as a reference.



695

696 **Fig. 6.** Validation of Approach A for the olive cultivar ‘Arbequina’ on the dataset of
 697 Experiment II. Predicted versus observed plots of fruit oil content (O_f) in relation to the 1:1
 698 line. Data are grouped in years (circles, squares and triangles for 2011, 2012 and 2013,
 699 respectively).

700



701

702 **Fig. 7.** Validation of Approach B for the olive cultivar ‘Arbequina’ on the dataset of
 703 Experiment II using three scenarios for the onset of oil accumulation: July 20th (A), August
 704 1st (B) and August 10th (C). Predicted versus observed plots of fruit oil content (O_f) in
 705 relation to the 1:1 line. Data are grouped in years (circles, squares and triangles for 2011,
 706 2012 and 2013, respectively).